Microsc. Microanal. Microstruct. **4** (1993) 137–142 APRIL/JUNE **1993**, PAGE 137

Classification
Physics Abstracts
61.16D — 81.20L — 61.80

Implantation of gold atoms into silicon by MeV electron irradiation

Hirotaro Mori([1]), Takao Sakata([1]), Masao Komatsu([1]) and Hidehiro Yasuda([2])

([1]) Research Center for Ultra-High Voltage Electron Microscopy, Osaka University, Yamadaoka, Suita, Osaka 565, Japan

([2]) Department of Materials Science and Engineering, Faculty of Engineering, Osaka University, Yamadaoka, Suita, Osaka 565, Japan

(Received January 18, 1993; accepted February 26, 1993)

Abstract. — Gold atom implantation into a silicon substrate, which is induced by MeV electron irradiation, has been examined by a combination of high voltage electron microscopy and high resolution electron microscopy. Gold atoms are implanted into the silicon substrate preferentially in the direction of incident electron beam. With increasing total dose of electrons gold-implanted regions become amorphous. With continued irradiation the amorphous gold-enriched region migrates in the substrate in the incident beam direction.

1. Introduction.

Nowadays foreign atom implantation into a solid is carried out mainly by ion implantation. This ion implantation has now matured into an indispensable part of semiconductor technology. However in this method, the introduction of foreign atoms is limited to regions or positions right beneath the free surface of the solid. Furthermore, severe cascade damages are inevitably caused in the implantation regions.

Recently, a unique, foreign-atom implantation technique in which irradiation effects of high energy (mega electron-volts) electrons are made use of, was proposed by Fujita. The outline of the technique is as follows [1, 2]. First, a dopant phase comprising a target element is deposited either on the surface or inside of the substrate. Here it is favorable that the target, dopant atom has a larger scattering cross-section for atom displacement than that of the solvent atom which constitutes the substrate. For example, such a combination of an element with a high atomic number and a low melting point as a dopant and another element with a low atomic number and a high melting point as a substrate will be preferred. The composite material is then irradiated with electrons having an energy greater than the corresponding threshold energy for atom displacement. Under irradiation the target atom in the dopant phase preferentially suffers elastic collisions with electrons and recoils with sufficient energy to intrude into the substrate. The repetition of the

intrusion will result in the implantation of the target atom into the substrate.

In this implantation technique, various advantages due to making use of electron beam as the primary irradiation beam can be fully utilized [3]. Namely, with the use of a microbeam of electrons, the implantation can be confined into a narrow region of the order of 2-3 nm in diameter. The implantation can be done without fear of contamination from the primary beam itself. Furthermore, the size and shape of the dopant-implanted region can precisely be controlled by changing the aperture angle of the electron beam. Therefore, by controlling these factors implantation can be performed on the surface or inside of a substrate material in a variety of scales. Through a systematic study by the authors' group, which has been carried out with the use of the 3 MV high voltage electron microscope (HVEM), it has been revealed that this technique is applicable not only to systems with metallic substrates but also to those with nonmetallic substrates [4-8].

In the present work, in an attempt to gain an insight into the mechanism behind the foreign-atom implantation into semiconductor substrates, gold atom implantation into a silicon substrate has been examined by a combination of HVEM and high resolution electron microscopy (HREM).

2. Experimental procedures.

Alloy ribbons of composition $Si_{99.8}Au_{0.2}$ were produced by quenching a previously melted button from the liquid state using a twin roller apparatus. Quenching was done in an argon atmosphere, and a roller speed of 6 m/s was used. The resultant alloy ribbons were approximately 50 μm in thickness, and the alloy contained a small amount of tiny gold particles which served as the target dopant phase. The ribbons were then mechanically polished to approximately 20 μm thickness, and disks of ca. 2 mm in diameter were cut out from the films. Final preparation of foil samples for transmission electron microscopy (TEM) was accomplished by a combination of the standard ion thinning and chemical etching techniques. In the latter technique a solution of 5 parts HNO_3 and 1 part HF was used as an etchant.

Electron irradiation experiments were carried out using a Hitachi HU-2000 type HVEM operated at 2 MV. Prior to irradiation, bright-field images (BFls) were taken from an area of a foil sample, as schematically shown in figure 1a. The foil sample was then rotated by 90 degrees along an axis vertical to the electron beam and was irradiated with 2 MeV electrons, as illustrated in figure 1b. The irradiation temperature and maximum flux of electrons were 170 K and $\sim 2.4 \times 10^{24}$ m^{-2} s^{-1}, respectively. After irradiation the foil sample was rotated by 90 degrees back to the original orientation, and BFls were taken from the same area, as depicted in figure 1c. In this manner a "cross-sectional" view of the irradiated area, as depicted in figure 1(c). In this manner a "cross-sectional" view of the irradiated area was obtained.

After irradiation experiments in the HVEM, the samples were transferred to a Hitachi H-9000 type HREM equipped with a tilting device ($\pm$ 10 degrees) and operating at 300 kV (Cs = 0.9 mm). High-resolution images were recorded under axial illumination at approximate Scherzer focus, with a point resolution better than 0.19 nm. The diameter of the objective aperture used was 20 μm which was large enough to include the 400 reflection of silicon. Optical diffraction patterns were taken from high-resolution negatives using a neon laser on an optical bench.

3. Results and discussion.

An example of gold-atom implantation which was induced by 2 MeV electron irradiation is shown in figure 2. Figure 2a is a BFI showing an area of a TEM sample before irradiation, and was taken

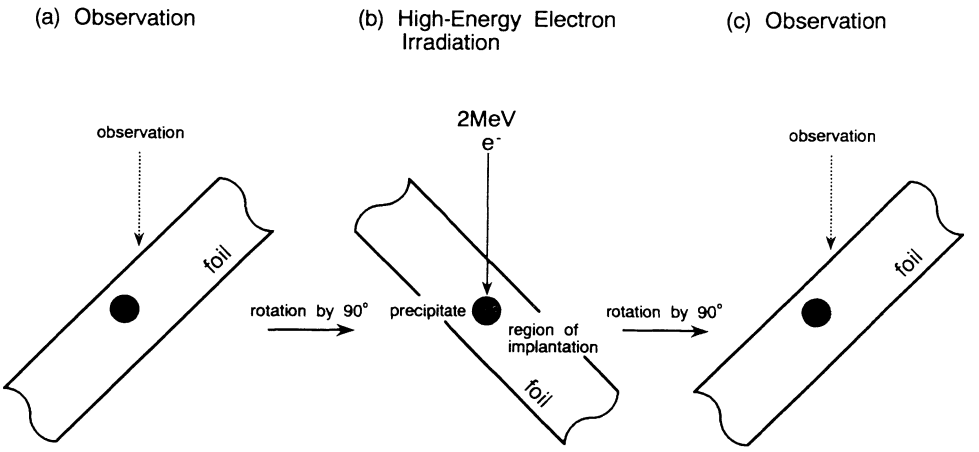

Fig. 1. — A schematic illustration of sample alignments for the "cross-sectional" observation of electron-irradiation-induced gold implantation. Figures (a), (b), and (c) depict sample alignments against the incident electron beam before, under, and after irradiation, respectively.

in the alignment illustrated in figure 1a. In this micrograph, gold particles which are embedded in the silicon matrix, appear dark. After taking this micrograph, the foil sample was rotated by 90 degrees and was irradiated with 2 MeV electrons for 7.2 ks in the alignment presented in figure 1b. During electron irradiation, a focussed beam of approximately 3 μm in diameter was always fixed at a position close to particle E. Since the flux profile of the electron beam was approximately Gaussian [9], a maximum total dose of electrons were deposited at a maximum flux on such particles as located close to particle E (i.e., particles B, C, E, and F) whereas a reduced total dose were deposited at a reduced flux on those far from particle E (i.e., particles G to I). After irradiation the foil sample was rotated back to the original orientation, and the same area as shown in figure 2a was observed in the alignment illustrated in figure 1c. The result obtained is depicted in figure 2b. The white arrows in figures 2a and b indicate a fixed position. The arrow labeled by letter e in figure 2b indicates the direction of 2 MeV electron beam used in the irradiation. It is clear from a comparison of figure 2a with b that particles A to F in figure 2a have migrated by this irradiation to positions A' to F' in figure 2b, respectively. The distance over which particles C and F have moved, is as long as 400 nm. Annealing experiments have revealed that not only particles seen at positions A' to F' but also such grey regions as produced in the wake of these particles are in an amorphous state. The grey contrast of these regions mainly comes from the difference in the atomic scattering factor between gold and silicon. On the other hand, as seen in figure 2b, particles on which a reduced total dose of electrons were deposited at a reduced flux (i.e., particles G to I) have shown no such migration of their centers of gravity and only regions which appears somewhat grey are produced at the back of these particles. The grey contrast of these regions again comes from the difference in the atomic scattering factor between gold and silicon. All these facts indicate that gold atoms are knocked off from target gold particles and are implanted into the silicon matrix, and the concentration profile of gold depends not only on the total dose of electrons but also on the flux.

Figure 3a is a high resolution electron micrograph of a gold-implanted region (double-arrowed) at an early stage of electron irradiation. The arrow marked by letter e in this figure again indicates the incident beam direction. It is evident from this micrograph that the gold-implanted region which extends at the back of the target gold particle (marked by letter T) is in an amorphous

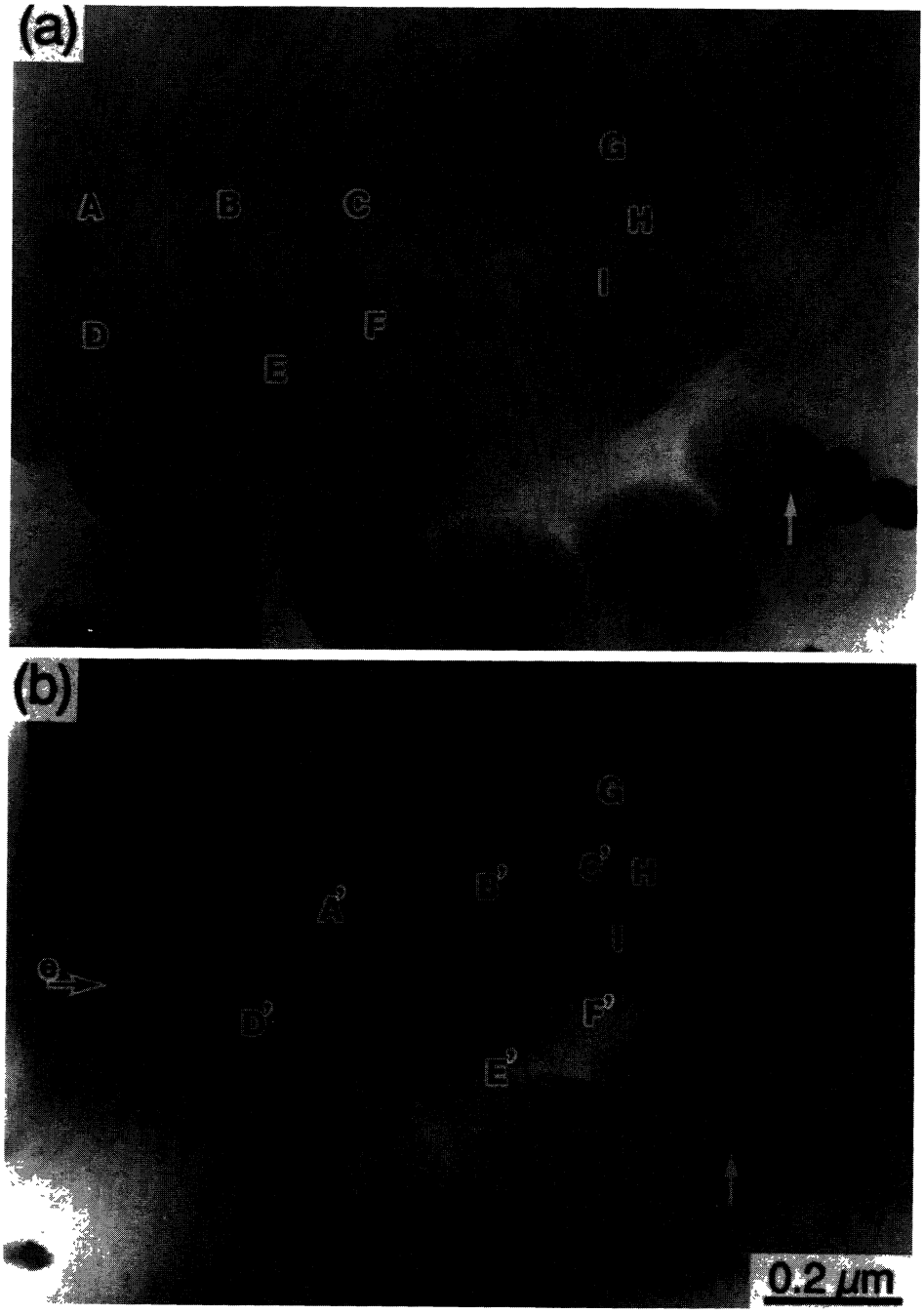

Fig. 2. — Gold atom implantation into silicon matrix induced by 2 MeV electron irradiation at 170 K with a maximum flux of $\sim 2.4 \times 10^{24} m^{-2} s^{-1}$. (a) before irradiation, (b) the same area as in (a) after 7.2 ks irradiation. The white arrows indicate a fixed position.

state. Figures 3b, c and d are optical diffraction patterns taken from areas which correspond to the target gold particle, the gold-implanted region, and the silicon matrix, respectively, in figure 3a. The optical diffractogram in figure 3d depicts a net pattern corresponding to the [110] zone axis diffraction pattern of silicon. The spots in the optical diffractogram in figure 3b are 111 systematic reflections of fcc gold. The optical diffractogram taken from the gold-implanted region (i.e., Fig. 3c) shows only an amorphous halo. A preliminary AES study of this amorphous phase has revealed that in this amorphous Au-Si alloy the p orbital of silicon forms a new p-d hybrid with the d orbital of gold [10].

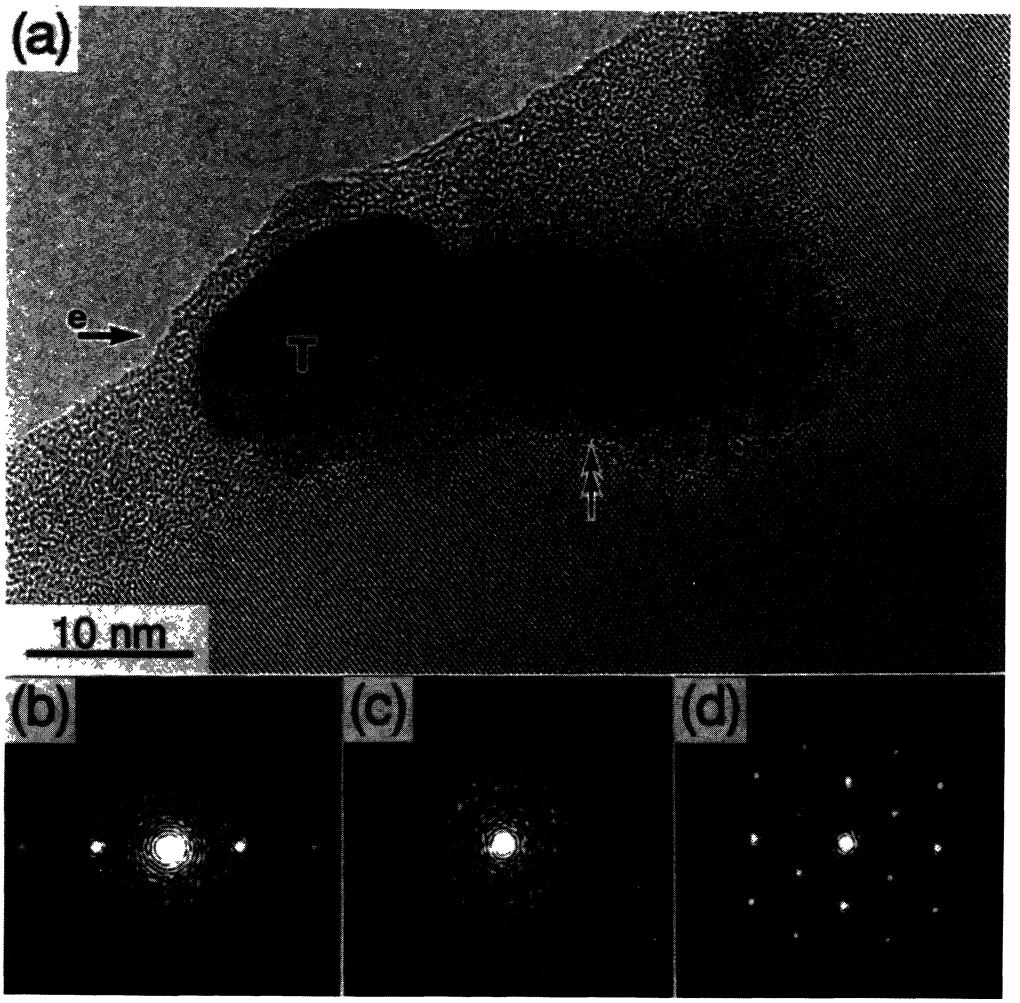

Fig. 3. — a) A high resolution electron micrograph showing the gold-implanted region (↟) which was formed at the back of a target gold particle (T). The arrow marked by letter e indicates the incident beam direction. The gold-implanted region is in an amorphous state. Figures (b), (c), and (d) are optical diffractograms taken from areas which correspond to the target gold particle, the gold-implanted region, and the silicon matrix, respectively, in figure (a).

From these results gold implantation into silicon by MeV electron irradiation is considered to take place in the following manner. Gold atoms in target gold particles preferentially suffer elastic collisions with MeV electrons and recoil with energies sufficient to intrude into the silicon substrate. The gold content in the gold-implanted region increases with increasing total dose of electrons, and eventually an amorphous Si-Au alloy is formed there in the gold-enriched region. In the amorphous Si-Au alloy, the sp^3 hybrid of silicon decays and a new bonding state is formed between silicon and gold, i.e., a type of silicide is formed. With continued irradiation, gold atoms in the amorphous alloy are repeatedly knocked-off and are subsequently implanted into the silicon substrate at somewhat deeper positions. The repetition of these displacements of gold atoms by the knock-on mechanism and subsequent silicide formation result in the deep implantation of gold into the silicon substrate.

4. Conclusions.

Gold atom implantation into a silicon substrate induced by MeV electron irradiation has been investigated by a combination of HVEM and HREM.

1) Gold atoms in target gold particles preferentially suffer elastic collisions with MeV electrons and recoil with energies sufficient to intrude into the silicon substrate. 2) The gold-implanted region eventually becomes amorphous. 3) With continued irradiation, gold atoms in the amorphous Si-Au alloy are repeatedly knocked-off and are subsequently implanted into the silicon substrate at somewhat deeper positions. 4) The repetition of these displacements of gold atoms by the knock-on mechanism and subsequent silicide formation result in the deep implantation of gold into the silicon substrate.

Acknowledgements.

The authors would like to thank Dr. K. Yoshida for his help in the maintenance of the HVEM. This work was supported in part by the Ministry of Education, Science and Culture, Japan, through Grant-in-Aid for Scientific Research on Priority Area.

References

[1] FUJITA H. and SUMIDA N., U.S. Patent No. 4668527 (1987).
[2] MORI H. and FUJITA H., U.S. Patent No. 4670291 (1987).
[3] MORI H., *J. Electron Microsc.* **38** (1989) 566.
[4] MORI H., NAKAMURA S. and FUJITA H., Proc. 11th Int. Congr. on Electron Microscopy, Kyoto, Japan, Aug. 31-Sept. 7, Eds. T. Imura, S. Maruse and T. Suzuki, published by Japanese *Soc. Electron Microsc.* (1986) p. 1113.
[5] FUJITA H. and MORI H., Proc. 5th Japan Inst. Metals Int. Symp. on Non-Equilibrium Solid Phases of Metals and Alloys, Kyoto, Japan, Mar. 14-17, published by Japan Inst. Metals (Sendai, 1988) p. 37.
[6] MORI H. and FUJITA H., Proc. Symposium on Advanced Materials, held in Osaka, Japan on February 5-7, Eds. H. Fujita and T. Imura, published by the Joint Committee for Advanced Materials Research (1990) p. 88.
[7] YASUDA H., SAKATA T. and MORI H., *Ultramicroscopy* **39** (1991) 321.
[8] MORI H., YASUDA H., SAKATA T. and FUJITA H., *Radiat. Eff. Defects Solids* **124** (1992) 51.
[9] MORI H., SAKATA T., FUJITA H. and INUI H., *Phil. Mag. Lett.* **61** (1990) 49.
[10] MORI H., YASUDA H., KOYAMA H., SUMIDA N. and FUJITA H., *Nucl. Instrum. Meth. B* **63** (1992) 291.